Elsevier Editorial System(tm) for Applied Clay Science

Manuscript Draft

Manuscript Number: CLAY12525R2

Title: Impact of particle size in serpentine thermal treatment: Implications for serpentine dissolution in aqueous-phase using CO2 in flue gas conditions.

Article Type: Research Paper

Keywords: Serpentine, Dehydroxylation; Particle Size; Heat Activation; X-Ray Diffraction Rietveld Refinement; Magnesium Leaching; Mineral Carbonation.

Corresponding Author: Dr. Louis-Cesar Pasquier, Ph.D.

Corresponding Author's Institution: Institut National de la Recherche Scientifique

First Author: Clémence Du Breuil

Order of Authors: Clémence Du Breuil; Louis-Cesar Pasquier, Ph.D.; Gregory Dipple; Jean-François Blais; Maria C Iliuta; Guy Mercier

Abstract: Mineral carbonation represents a promising way of reducing the emission of anthropogenic GHG emissions, particularly in the Province of Québec where large amounts of serpentine mining residues are waiting for remediation. However, when used in reactors, serpentine minerals need to be activated to promote Mg2+ leaching. In this study, ground and unground samples have been thermally activated in a muffle furnace at different temperatures and residence times. Their mineralogical composition have been determined using XRD coupled with Rietveld refinements from which the amorphous phases have been distinguished and quantified. The objectives are to determine the influence of the particle size distribution of the samples on the dehydroxylation process and on the dissolution under aqueous mineral carbonation reaction. Results show that in a muffle furnace, unground particles tend to heat faster than ground particles. This is due to the larger spaces left between the particles, allowing a better heat diffusion through the sample. In ground particles samples, water vapor tends to be entrapped in those space, leading to the formation of a water vapor layer, slowing down the heat process. Carbonation experiments were performed on the different resulting fractions obtained. Regarding Mg dissolution efficiencies, 6 batches experiments show that Mg2+ extraction is higher when performed on sample ground prior to thermal activation. The collected information will advance the knowledge on serpentine heat activation mechanism and help to improve carbonation technologies efficiencies.

Response to Reviewers: Mineral carbonation represents a promising way of reducing the emission of anthropogenic GHG emissions, particularly in the Province of Québec where large amounts of serpentine mining residues are waiting for remediation. However, when used in reactors, serpentine minerals need to be activated to promote Mg2+ leaching. In this study, ground and unground samples have been thermally activated in a muffle furnace at different temperatures and residence times. Their

mineralogical composition have been determined using XRD coupled with Rietveld refinements from which the amorphous phases have been distinguished and quantified. The objectives are to determine the influence of the particle size distribution of the samples on the dehydroxylation process and on the dissolution under aqueous mineral carbonation reaction. Results show that in a muffle furnace, unground particles tend to heat faster than ground particles. This is due to the larger spaces left between the particles, allowing a better heat diffusion through the sample. In ground particles samples, water vapor tends to be entrapped in those space, leading to the formation of a water vapor layer, slowing down the heat process. Carbonation experiments were performed on the different resulting fractions obtained. Regarding Mg dissolution efficiencies, 6 batches experiments show that Mg2+ extraction is higher when performed on sample ground prior to thermal activation. The collected information will advance the knowledge on serpentine heat activation mechanism and help to improve carbonation technologies efficiencies.

Research Data Related to this Submission

There are no linked research data sets for this submission. The following reason is given:
Data will be made available on request

Impact of particle size in serpentine thermal treatment: Implications for serpentine dissolution in aqueous-phase using CO_2 in flue gas conditions

Clémence Du Breuil [a], Louis César Pasquier [b,*], Gregory Dipple [c], Jean-François Blais [d], Maria Cornelia Iliuta [e], Guy Mercier [f]

[a] Ph.D. Student, Institut National de la Recherche Scientifique (Centre Eau, Terre et Environnement), Université du Québec, 490 rue de la Couronne, Québec, QC, Canada, G1K 9A9, Phone: (418) 654-2550, Fax: (418) 654-2600, email: clemence.jouveau_du_breuil@inrs.ca

[b] Professor, Institut National de la Recherche Scientifique (Centre Eau, Terre et Environnement), Université du Québec, 490 rue de la Couronne, Québec, QC, Canada, G1K 9A9, Phone: (418) 654-2633, Fax: (418) 654-2606, email: louis-cesar.pasquier@ete.inrs.ca

[c] Professor, University of British Columbia, Department of Earth, Ocean and Atmospheric Sciences, 2020 – 2207 Main Mall, Vancouver, BC Canada V6T 1Z4, Phone: (604) 827-0653, email: gdipple@eoas.ubc.ca

[d] Professor, Institut National de la Recherche Scientifique (Centre Eau, Terre et Environnement), Université du Québec, 490 rue de la Couronne, Québec, QC, Canada, G1K 9A9, Phone: (418) 654-2541, Fax: (418) 654-2600, email: jean-francois.blais@ete.inrs.ca

[e] Professor, Université Laval, Chemical Engineering Department, Québec, QC, Canada, G1V 0A6, Phone: (418) 656-2204, Fax: (418) 656-5993, email: maria-cornelia.iliuta@gch.ulaval.ca

[f] Professor, Institut National de la Recherche Scientifique (Centre Eau, Terre et Environnement), Université du Québec, 490 rue de la Couronne, Québec, QC, Canada, G1K 9A9, Phone: (418) 654-2633, Fax: (418) 654-2600, email: guy.mercier@ete.inrs.ca

[*] Corresponding Author

1 INTRODUCTION

Greenhouse gas emissions including anthropogenic CO_2 is disrupting the climate (IPCC, 2018), and mineral carbonation is one of the most valuable remediation solutions (Seifritz, 1990; Lackner et al., 1995).It is a spontaneous and exothermic reaction that occurs naturally between atmospheric CO_2 and divalent cation-bearing silicates.

Serpentines are attractive reactants due to their high magnesium content—up to 40 wt % (Page, 1968). Moreover, their high availability and abundance in the Province of Quebec represents their great potential for such a process (Huot et al., 2003). Three main polymorphs—chrysotile, lizardite, and antigorite—constitute the serpentine minerals groups ($Mg_3Si_2O_5(OH)_4$). Their structure is a stack of layers composed of two sheets: a tetrahedral sheet composed of silica tetrahedron (SiO_4) linked by their apical oxygen to an octahedral sheet composed of $Mg(OH)_2$ (Aruja, 1945; Nagy and Faust, 1956; Wicks and Whittaker, 1977). Van der Waals interactions ensure interfoliar cohesion via the outer hydroxyl groups, and intrafoliar cohesion is due to the inner hydroxyl groups (Mellini and Zanazzi, 1987; Turci et al., 2008; Larachi et al., 2010).

At high temperatures, serpentine minerals undergo dehydroxylation. Serpentines can lose up to 14 wt % of their initial mass depending on their initial water content (Jolicoeur and Duchesne, 1981; Turci et al., 2008). At the beginning of the process (between 100 ºC and 300 ºC) the non-structurally bonded water molecules escape the structure. As the temperature increases, a pseudo-amorphous serpentine, α-metaserpentine is formed and corresponds to 50 % of the total dehydroxylation reaction. When it reaches 90 % of the total dehydroxylation reaction, a meta-serpentine partially replaces the initial structure. Beyond 700 ºC, forsterite starts to crystalize and is joined by enstatite after

875 ºC (Hey and Bannister, 1948; Ball and Taylor, 1963; Brindley and Hayami, 1963, 1965; Gualtieri et al., 2012).

The magnesium atoms are linked to hydroxyls inside the structure. Thus, it is important to heat treat the serpentine prior to dissolution. This enhances magnesium leaching and improves material dissolution to promote CO_2 carbonation (Lackner et al., 1995). Alternatives to heat activation proposes pH swing processes, where cations are exctracted using strong acids or ammonium salts. Carbonates are then precipitated after increasing the pH using base (Park and Fan, 2004; Teir et al., 2007; Wang and Maroto-Valer, 2011; Azdarpour et al., 2015; Lacinska et al., 2016; Ferrufino et al., 2018). Mechanical and microwaves applications were also tested (Kim and Chung, 2002b; Yoo et al., 2009; Bobicki et al., 2014; Li and Hitch, 2016).

Thermal activation of the serpentine has been thoroughly investigated in previous studies and linked to dissolution efficiency under carbonation reaction conditions (Gerdemann et al., 2003; O'Connor et al., 2005; Li et al., 2009; Mann, 2014; Lacinska et al., 2016). Serpentine dissolution—and thus magnesium availability—is a carbonation-reaction limiting factor. It is mostly controlled by the efficiency of the thermal activation. In addition, the formation of meta-serpentine promotes Mg^{2+} leaching during carbonation (Mckelvy et al., 2004). The proportion of Mg^{2+} leached during the dissolution part of the carbonation reaction is used here to evaluate the efficiency of the thermal activation. Therefore, no carbonates were precipitated from the solution. The leaching conditions used are similar to those described and investigated by Pasquier et al. (2014b).

A few studies have evaluated the impact of grain size distribution during thermal activation on carbonation: Alexander et al. (2007) showed that finely ground materials are required to achieve a higher yield of carbonation. Other studies (Martinez, 1961;

Drief and Nieto, 1999; Hrsak et al., 2008) investigated the impact of grinding on thermal treatment in terms of dehydroxylation. Grinding affects the thermal treatment of chrysotile by decreasing the dehydroxylation temperatures. Therefore, the loss of mass due to dehydroxylation starts at lower temperature in the ground sample; this decreases the temperature of formation of the amorphous phases and forsterite. The octahedral layers preferentially break into ground particles (Drief and Nieto, 1999).

Dehydroxylation in ground particles can be enhanced by two factors: (i) the increase in surface area resulting from grinding can favor escape of hydroxyl groups; (ii) the alteration of bonds during grinding allows them to break at lower temperatures. This again helps the hydroxyl groups escape the structure. Water vapor would form between the particles once the hydroxyl groups are no longer bound to the structure. In finely ground materials, the compaction of particles leads to entrapment that releases water vapor and inhibits liberation from the material (Brindley and Hayami, 1965; Dlugogorski and Balucan, 2014). Several studies have evaluated the potential of serpentine mechanical activation via grinding as a tool to promote carbonation. The results show that a prolonged grinding (120 minutes) can greatly enhance the extraction of metals from the serpentine structure and improve carbonation efficiency (Kim and Chung, 2002a; Li and Hitch, 2015; Rigopoulos et al., 2018). Bloise et al. (2018) observed a shift to lower temperature in the dehydroxylation process—this decreased its enthalpy and encouraged evaluation of the grinding impact on thermal activation.

This study extends research on cement plant direct flue gas mineral carbonation by Mercier et al. (2016) at INRS, Québec, using optimized the reaction conditions and demonstrated the economic viability and overall feasibility of the process for the Province of Québec (Pasquier et al., 2014a; Pasquier et al., 2016). The final stage of the process is precipitation of carbonates, and this was studied in detail by Moreno Correia

(2018). A pilot scale test conducted in 2015 highlighted the importance of optimizing thermal treatment conditions for the INRS process (Kemache et al., 2016; Kemache et al., 2017). Previous unpublished work from the group determined them to be 750 °C for a treatment of 15 minutes using a static conventional furnace with a mineralogical assemblage of intermediate amorphous phases and meta-serpentine materials.

The particles size distribution is critical for process reliability and carbonation. In addition to temperature and residence time, it enables a better understanding of serpentine thermal activation and can provide insights on how it affects the dissolution of the serpentine. This paper provides a better understanding of the process behind heat diffusion within the particles during static prograde thermal treatment. The temperature at which the mineral transformations occurred during dehydroxylation of ground and unground serpentine was observed using a novel approach to quantify amorphous phases. We also evaluated the role of particle size distribution on thermal activation and its impact on Mg dissolution under flue gas carbonation conditions.

2 MATERIAL AND METHODS

2.1 Material

The residues used here come from Jeffrey Mine, in the town of Asbestos in Southern Québec. The material sampled was already crushed and have a sand like appearance with a mean granulometry of 416 µm (Figure 1). The remaining fibers were removed for sanitary precautions by flottating them in water. About 90 wt % of the iron oxides were separated by density using a Wilfley table due to their potential commercial value and poor carbonation behavior. The resulting material is corresponding to the initial and unground sample discussed within the manuscript.

The chemical composition of liquid and solids were obtained with inductively coupled plasma-atomic emission spectrometry (ICP-AES) after being fused using lithium metaborate via the Claisse Method. The starting composition of the residue is given in table 1. The chemical composition is consistent with previously analyzed samples collected in the area. Loss on ignition for both samples (ground and unground) were measured via heating at 1 025 °C for 6 h; the samples were 13.9 wt % for the ground sample and 13.2 wt % for the unground sample.

Table 1

2.2 Physical characterization

Half of the residue was ground using a ring mill (Retsch RS200) to obtain a mean size of 28 µm. The unground sample presented a mean particle size of 416 µm. The particle size distribution was measured with a particle size distribution analyzer LA-950V2 Horiba. Figure 1 present the granulometry curve of both ground and unground samples. Specific surface areas (SSA) were obtained via N2 adsorption at ambient temperature using Brunauer–Emmett–Teller methodology (BET) (Brunauer et al., 1938) (table 2).

Figure 1

Table 2

2.3 Phases identification and quantification

X-Ray diffraction (XRD) was performed using a Siemens D5000 Bragg-Brentano Θ-2Θ diffractometer with CuKα radiation (40 kV, 40 mA). An aliquot of 1.6 g of each sample was mixed with 0.4 g of pure corundum (Al_2O_3) acting as a 20.0 wt % spike. To ensure homogenization, samples were ground in ethanol using agate grinding pellets for 7

minutes in a McCrone micronizing mill. Scans were acquired for 30 minutes with 2Θ values of 3° to 80° with a scanning step size of 2Θ = 0.3° and a counting time of 7 seconds per step. Matches were identified using Brucker identification software DIFFRACplus EVA and the ICDD PDF-2 database. Phase quantification was performed using the Rietveld method (Bish & Howard, 1988; Pawley, 1981; Raudsepp et al., 1999; Rietveld, 1969). This method is based on a calibration factor derived from the mass and volume of each phase's unit cell, and it requires all phases to present a high crystallinity level and a well-defined crystal structure. However, serpentine minerals show discrepancies from their ideal structure (Turvey et al., 2017; Wilson et al., 2006) and require the use of the partial or not known crystalline structure (the PONKCS method) (Scarlett & Madsen, 2006). A calibrated mass value (Rietveld, 1969) leads to chrysotile peak fitting (Le Bail, 2005); the unit cell parameters and space group (Falini et al., 2004) calibrated the PONKCS model. A standard sample of pure chrysotile and fluorite have well-known proportions and are used for this calibration (Wilson et al., 2006). The PONKCS file can then be used as a crystallographic information file in TOPAS software from Bruker. The results show two amorphous phases—intermediate amorphous components and meta-serpentine materials (see supplementary materials).

2.4 Thermal treatment

2.4.1 Prograde tests

Prograde heating tests used a Neyo M-525 Series II muffle furnace. Two thermocouples using type K probes were inserted inside the furnace—one measured the temperature inside the furnace and the other measured the temperature inside the sample. Ground and unground samples were tested. Forty grams of sample were placed in a cast-iron skillet 10 cm diameter and 4 cm depth. The sample temperature measuring probe was

insert inside the powder 3 to 4 cm deep to obtain its core temperature. The calibration curve is given in figure 2. Both temperatures were measured every two minutes until both reached 750 ºC.

Figure 2

2.4.2 Isothermal tests

Isothermal treatments were performed in batch mode using a Furnatrol I33 muffle furnace (Thermolyne Subron Corporation). A cast iron skillet 20 cm diameter and 4 cm deep containing 20 g of sample was placed in the furnace and set beforehand to the test temperature. A range of temperatures (500 ºC, 650 ºC and 750 ºC) were tested every 15, 30, and 60 min. Samples were weighed before and after the test, and the variation corresponded to the mass loss.

2.5 Successive batches dissolution

Dissolution tests used the carbonation conditions optimized by Pasquier et al. (2014a). These were performed in a 300-mL stirred reactor (model 4561; Parr Instrument Company) using 4.0 vol % O_2 and 18.2 vol % CO_2 balanced with N_2. This simulates the flue gas of a cement plant at 22 ºC ± 3 ºC. The solid ratio was set to 15 wt % (150 $g.L^{-1}$). A batch of gas at 10.2 bar was injected in the reactor and reacted for 15 minutes under an agitation of 600 rpm. During the experiment, the pressure dropped to 0.1 from 3.5 bar depending on the amount of gas initially inserted. At the end of the first batch, the gas was emptied from the reactor, and 10.2 bar of gas was re-injected for a second 15-minutes batch. The pulp was filtered every two batches, and the liquid phase was acidified using 50 % nitric acid and sampled for chemical analyses. After 6 batches, the solid was dried at 60 °C and ground using a ring mill at 700 RPM for 1 min to remove the

silica passivation layer formed around the particles. This was then used for another six batches. Depending on the tests, the solid was tested for 2, 6, or 12 batches to follow the leaching efficiency along successive CO_2 injections (figure 3).

The efficiency of thermal activation was observed as magnesium leached from the solid during the reaction. Reliability in the method was endorsed by performing mass balance to highlight any precipitation occurring during manipulation or during the pressure release of the vessel. This efficiency was studied using equation 1 where $[Mg]_{liq}$ is the measured concentration of Mg^{2+} in the final solution, V and m are the volume of solution and the mass of solid, respectively, and C_{Mg} is the concentration of magnesium in the solid measured after thermal treatment. Carbonates did not precipitate from the solution.

Equation 1 Proportion of Mg^{2+} leached

$$\%Mg = ([Mg]_{liq} * V) / (C_{Mg} * m)$$

Figure 3

2.6 Approach

Two tests were performed and compared to tests performed on ground samples. Treated and ground samples were first thermally-treated and then ground for dissolution under carbonation conditions; ground samples are ground prior to thermal treatment and then submitted to dissolution. Unground samples were directly considered for dissolution. Dissolution of untreated samples used two batches of gas (figure 4).

Figure 4

3 RESULTS

3.1 Heat diffusion during prograde heating

Figure 5 shows the temperature inside the ground and unground samples as well the furnace temperature. It represents heat diffusion speed inside the two tested samples and inside the furnace.

Figure 5

Both samples reached the expected temperature at the end of the experiment. However, it appears that the heat diffuses faster inside the unground particles. The line corresponding to the temperature inside unground particles (figure 5) shifted to the left meaning that this sample reaches this temperature sooner than the ground sample.

Figure 6

Figure 6 present the heating speed within the furnace. The difference between the two samples is more evident as the heating rate is higher in unground particles than in fine particles. On both figures, the lag between the furnace and sample temperature is clearly shown. Furnace temperature is quickly increasing within the first 10 minutes, up to 35 °C. min^{-1}. Then it quickly falls down to show a steady decrease until the end. Heating rates on samples are less hectic. It rapidly increases to reach a high plateau around 20 °C. min^{-1} and 10 minutes. Before 20 minutes the rate slowly decreases and join the furnace rate after 50 minutes.

3.2 Thermal activation

3.2.1 Mass loss

Figure 7 compares the mass lost during isothermal treatment of ground (x-axis) and unground (y-axis) particles. The dotted line represents the 1:1 line where the mass lost by ground and unground particles are equal. Most samples are on the right side of this line illustrating that ground samples present a higher mass loss. As expected, increasing the temperature is inducing a higher mass loss. The same pattern is observed with the time.

Figure 7

3.2.2 Mineralogical transformations

The starting materials are mostly serpentine and magnetite (table 3). The amorphous phase was quantified using the Rietveld method, but this is the result of the stacking disorder observed in the serpentine structure (Wilson et al., 2006; Turvey et al., 2017). Nevertheless, the original data shows the Rietveld refinements and indicates that the measured amorphous phase proportion differs from one sample to the other. Indeed, the grinding performed to obtain the fine sample induced 6.2 wt % of amorphous to start with.

Table 3

As previously demonstrated, the thermal treatment of serpentine minerals leads to a series of mineralogical transformations. Transformations in fine particle serpentine samples have been studied in a previous study (table 4 (ground)). These data are compared to those in unground particles (unground). Intermediate amorphous phases

tend to form faster in ground particles versus unground samples. Treatment at 550 °C for 15 min led to 36.8 g of product per 100 g of starting material; unground sample similarly treated only presents 14.4 g per 100 g of starting material. The grinding-induced amorphization observed in the ground starting material might lead to the formation of intermediate amorphous phases at lower temperatures (as low as 500 °C). The meta-serpentine phase appears earlier in the unground particles (550 °C for 15 minutes) versus 650 °C at 15 minutes in ground particles.

Forsterite starts to crystallize at 650 °C for 60 minutes in unground particles as a result of the dehydroxylation reaction with 5.0 g/100 g of starting material while the ground one displays 2.1 g per 100 g of starting material. The formation of forsterite was observed with 750 °C treatment for 30 minutes on ground particles; the yield is higher (24.8 g per 100 g of starting material). At 650 °C for 30 minutes, the mineral distribution is similar in ground and unground samples with intermediate amorphous phases representing more than half of the samples: meta-serpentine and residual serpentine. Furthermore, the content of meta-serpentine samples formed at 750 °C for 15 minutes in both ground and unground particles are different (26.8 and 5.5 g per 100 g of starting material, respectively); the unground sample produced 34.0 g per 100 g of starting material of forsterite. The formation of hematite partially results from the oxidation of serpentine iron and magnetite. It is less common in unground particles.

Table 4

3.3 Dissolution of thermally-treated serpentine

Figure 8 show the results of successive batches dissolution tests performed on untreated and thermally-treated samples (isothermal treatments). Each sample was divided into three experiments: (i) unground, (ii) ground prior to thermal activation, and

(iii) ground after thermal activation. Hatching patterns (thermally-treated unground and untreated samples) represent an extrapolation of the proportion of Mg^{2+} extracted after twelve batches of gas treatment. Thermally-treated ground samples were tested in twelve batches, and six batches of thermally-treated unground samples were tested; two batches of untreated samples were tested. Extrapolation was computed based on the average proportion of Mg^{2+} extracted during the next six to ten batches for samples tested for twelve batches and applied to the considered samples.

Overall, it appears that dissolution performed on fine particles—in terms of the amount of Mg^{2+} extracted—offers better results than those performed on unground or post-treatment ground particles (Pasquier et al., 2014a). Untreated samples have a much lower proportion of leached Mg^{2+} because thermal treatment is required to enhanced serpentine dissolution (Lackner et al., 1995). Despite their low amount of Mg^{2+}, the proportion is higher (6.8 %) for ground particles than for unground particles (2.1 %).

The samples on which dissolution was performed after grinding showed similar results: close to 30 % of Mg^{2+} extracted after twelve batches of CO_2, except for the one treated at 750 °C for 15 minutes which reached 45 % of Mg^{2+} extracted. For treatment at 650 °C during 30 minutes, results show that particle size does not affect the extraction of Mg^{2+} as both ground and post-treated ground sample leached close to 30 % of magnesium after twelve batches of gas.

Figure 8

BET measurements performed on thermally-treated ground and unground samples (table 5) showed that the specific surface area (SSA) varies with the temperature and duration of the treatment. The SSA of a ground sample treated at 650 °C for 30 minutes decreases versus a ground untreated sample. In contrast to prior reports Larachi et al.

(2010), as the temperature increases, the SSA drastically increases to 31.04 $m^2.g^{-1}$ for a ground sample treated at 750 °C for 15 minutes. Therefore, the enhanced dissolution of material treated at 750 °C for 15 minutes might be due to both a suitable mineralogy and a higher specific surface area. This suggests that thermal treatment makes the particles increasingly porous as the amorphous phases are formed. Unground particles treated at 750 °C have a significant increase in their SSA while unground particles treated at 650 °C for 30 minutes show a significant drop. This can be due to the smaller amount of meta-serpentine within the samples treated at 750°C compared to the samples obtained at 650°C after 30 minutes.

Table 5

4 DISCUSSION

Forsterite and amorphous phases tend to crystalize sooner in unground samples than in ground samples indicating a shift in the dehydroxylation temperatures according to particle size. Mineralogical transformations which should occur at temperatures higher than 750 ˚C as seen in ground particles, tend to occur at much lower temperature or for shorter residence times in unground samples. Therefore, two important aspects are observed: (i) the role of grinding on breaking down the serpentine structure; and (ii) the influence of the particles size and compaction of the grains on the water vapor diffusion during heating.

Brindley and Hayami (1965) showed that grinding tends to slow down the crystallization rate of the dehydroxylation products (forsterite and enstatite). The dehydroxylation reaction is topotactic (Aruja, 1945), and the formation of products will be delayed if the atomic positions are disrupted by grinding. These observations contrast with those made by Drief and Nieto (1999) who demonstrated that the dehydroxylation reaction can be

hastened with grinding due to the transformation of structurally-bound water into surface-absorbed water. Furthermore, Martinez (1961) noted a decrease in the starting temperatures for dehydroxylation when the serpentine minerals are ground suggesting that the dehydroxylation stages are reached sooner in ground particles. This may be caused by an increase in the specific surface area during grinding, which offers a larger surface for the hydroxyl groups to escape the structure. However, a higher specific surface area also induced a higher compaction of particles; hence, there is less space between the samples.

Dlugogorski and Balucan (2014) suggested that dense and compact particles would prevent hydroxyl groups from being released as water vapor and thus escaping the particles. Seipold and Schilling (2003) assumed that the two heat flow mechanism should be considered during serpentine heating. Heat must be transported by both (i) heat conduction and (ii) heat advection. The second supposes that a part of the heat is carried advectively by water vapor throughout the particles. Therefore, water vapor disposes of larger spaces between the particles in unground samples. They circulate and heat the sample.

In ground samples, the water vapor cannot travel as easily inside the spaces left between the particles. They are smaller and are less connected than in unground samples. This leads to an accumulation of water vapor in those spaces. This might lead to the formation of a thin film around the particles as described by the Ledeinfrost effect—this delays the dehydroxylation process.

Furthermore, the fact that the heat diffusion is slower when treatment is performed on a ground sample might be due to the experimental set-up. Previous observations suggested that thermal treatments performed in a static furnace fostered the entrapment

of water vapor between the particles leading to a shift in the dehydroxylation temperatures. Dlugogorski and Balucan (2014) suggested that when dealing with dense and compacted fine particles, they should be fluidized to avoid such entrapment. Our observations confirm this. Therefore, thermal treatments should be performed dynamically such as in a rotary kiln or with a fluidized bed. This would help the released water pressure to escape from the structure.

The onset of the dehydroxylation process would occur at lower temperatures or within a shorter treatment time than in a static experimental set-up. Furthermore, when optimizing the thermal treatment step in a mineral carbonation process, the grinding place should be thoroughly investigated. This study highlights the impact of the type of furnace used for activation. Samples should be ground prior to thermal treatment when using a conventional static furnace. This prevents formation of forsterite and promotes the formation of amorphous phases.

5 CONCLUSIONS

In this paper, the influence of particles size on serpentine thermal activation for dissolution under direct flue gas carbonation was explored to better explain its impact. The following conclusions can be drawn:

- When a static treatment is performed on particles, coarser ones tend to heat faster because there is more space available between them for the heat to circulate. In fine particles, water molecules escaping the structure are trapped between the particles and form a layer between them. Therefore, the dehydroxylation process is slowed down under these thermal treatment conditions.

- Samples treated at 750 °C for 15 minutes show a significant increase in its specific surface area. These are combined with a suitable mineralogical assemblage that leads to a better dissolution of the material. Unground particles showed a similar trend in variation of their SSA as ground particles.
- Formation of amorphous phases including products of the dehydroxylation reaction is enhanced by grinding due to the preliminary disruption of the crystalline structure.
- Dissolution of serpentine under carbonation specific condition is improved when thermal activation is performed on fine particles rather than on unground particles in a static furnace.

ACKNOWLEDGMENTS

This research was funded by ‘Projet de recherche en équipe’ grant from FRQNT. The authors would like to thank Greg Dipple’s and Matti Raudsepp’s teams of UBC (Vancouver) for their advice and help on the XRD and Rietveld refinement application to the serpentine minerals as well as Université Laval (Québec) for performing the BET measurements.

REFERENCES

Alexander, G., Maroto-Valer, M.M., Gafarova-Aksoy, P., 2007. Evaluation of reaction variables in the dissolution of serpentine for mineral carbonation. Fuel 86, 273-281.

Aruja, E., 1945. An X-ray study of the crystal-structure of antigorite (With Plate V). Mineralogical Magazine and Journal of the Mineralogical Society 27, 65-74.

Azdarpour, A., Asadullah, M., Mohammadian, E., Hamidi, H., Junin, R., Karaei, M.A., 2015. A review on carbon dioxide mineral carbonation through pH-swing process. Chem Eng J 279, 615-630.

Ball, M., Taylor, H., 1963. The dehydration of chrysotile in air and under hydrothermal conditions. Mineralogical Magazine 33, 467-482.

Bloise, A., Catalano, M., Gualtieri, A., 2018. Effect of grinding on chrysotile, amosite and crocidolite and implications for thermal treatment. Minerals-Basel 8, 135.

Bobicki, E.R., Liu, Q., Xu, Z., 2014. Microwave heating of ultramafic nickel ores and mineralogical effects. Miner Eng 58, 22-25.

Brindley, G., Hayami, R., 1963. Kinetics and Mechanisms of Dehydration and Recrystallization of Serpentine—I. Clays and Clay minerals 12, 35-47.

Brindley, G., Hayami, R., 1965. Mechanism of formation of forsterite and enstatite from serpentine. Mineralogical Magazine and Journal of the Mineralogical Society 35, 189-195.

Dlugogorski, B.Z., Balucan, R.D., 2014. Dehydroxylation of serpentine minerals: Implications for mineral carbonation. Renew Sust Energ Rev 31, 353-367.

Drief, A., Nieto, F., 1999. The effect of dry grinding on antigorite from Mulhacen, Spain. Clays and Clay Minerals 47, 417-424.

Ferrufino, G.L.A., Okamoto, S., Dos Santos, J.C., de Carvalho, J.A., Avila, I., Luna, C.M.R., Neto, T.G.S., 2018. CO2 sequestration by pH-swing mineral carbonation based on HCl/NH4OH system using iron-rich lizardite 1T. Journal of Co2 Utilization 24, 164-173.

Gerdemann, S.J., Dahlin, D.C., O'Connor, W.K., Penner, L.R., 2003. Carbon dioxide sequestration by aqueous mineral carbonation of magnesium silicate minerals, Greenhouse gas technologies. Albany Research Center (ARC), Albany, OR, US, p. 8.

Gualtieri, A.F., Giacobbe, C., Viti, C., 2012. The dehydroxylation of serpentine group minerals. Am Mineral 97, 666-680.

Hey, M., Bannister, F., 1948. A note on the thermal decomposition of chrysotile. Mineralogical Magazine and Journal of the Mineralogical Society 28, 333-337.

Hrsak, D., Sucik, L., Lazic, L., 2008. The thermophysical properties of serpentinite. Metalurgija 47, 29-31.

Huot, F., Beaudoin, G., Hébert, R., Constantin, M., Dipple, G.M., Raudsepp, M., 2003. Le piegeage du CO_2 anthropique dans les parcs à résidus d'amiante du sud du Québec: Concept et valorisation. Rapport Université Laval, Qc, Canada. 167p.

IPCC, 2018. GLOBAL WARMING OF 1.5 °C, an IPCC special report on the impacts of global warming of 1.5 °C above pre-industrial levels and related global greenhouse gas emission pathways, in the context of strengthening the global response to the threat of climate change, sustainable development, and efforts to eradicate poverty, p. 34.

Jolicoeur, C., Duchesne, D., 1981. Infrared and thermogravimetric studies of the thermal degradation of chrysotile asbestos fibers: evidence for matrix effects. Canadian Journal of Chemistry 59, 1521-1526.

Kemache, N., Pasquier, L.-C., Cecchi, E., Mouedhen, I., Blais, J.-F., Mercier, G., 2017. Aqueous mineral carbonation for CO 2 sequestration: From laboratory to pilot scale. Fuel Processing Technology 166, 209-216.

Kemache, N., Pasquier, L.-C., Mouedhen, I., Cecchi, E., Blais, J.-F., Mercier, G., 2016. Aqueous mineral carbonation of serpentinite on a pilot scale: The effect of liquid recirculation on CO2 sequestration and carbonate precipitation. Appl Geochem 67, 21-29.

Kim, D.-J., Chung, H.-S., 2002a. Effect of grinding on the structure and chemical extraction of metals from serpentine. Particulate science and technology 20, 159-168.

Kim, D.J., Chung, H.S., 2002b. Effect of grinding on the structure and chemical extraction of metals from serpentine. Particulate Science and Technology 20, 159-168.

Lacinska, A.M., Styles, M.T., Bateman, K., Wagner, D., Hall, M.R., Gowing, C., Brown, P.D., 2016. Acid-dissolution of antigorite, chrysotile and lizardite for ex situ carbon capture and storage by mineralisation. Chem Geol 437, 153-169.

Lackner, K.S., Wendt, C.H., Butt, D.P., Joyce, B.L., Sharp, D.H., 1995. Carbon dioxide disposal in carbonate minerals. Energy 20, 1153-1170.

Larachi, F., Daldoul, I., Beaudoin, G., 2010. Fixation of CO2 by chrysotile in low-pressure dry and moist carbonation: Ex-situ and in-situ characterizations. Geochimica Et Cosmochimica Acta 74, 3051-3075.

Li, J., Hitch, M., 2016. Mechanical activation of ultramafic mine waste rock in dry condition for enhanced mineral carbonation. Miner Eng 95, 1-4.

Li, J.J., Hitch, M., 2015. Ultra-fine grinding and mechanical activation of mine waste rock using a high-speed stirred mill for mineral carbonation. Int J Min Met Mater 22, 1005-1016.

Li, W.Z., Li, W., Lia, B.Q., Bai, Z.Q., 2009. Electrolysis and heat pretreatment methods to promote CO2 sequestration by mineral carbonation. Chem Eng Res Des 87, 210-215.

Mann, J.P., 2014. Serpentine Activation for CO2 Sequestration.

Martinez, E., 1961. The effect of particle size on the thermal properties of serpentine minerals. American Mineralogist: Journal of Earth and Planetary Materials 46, 901-912.

Mckelvy, M.J., Chizmeshya, A.V.G., Diefenbacher, J., Bearat, H., Wolf, G., 2004. Exploration of the role of heat activation in enhancing serpentine carbon sequestration reactions. Environ Sci Technol 38, 6897-6903.

Mellini, M., Zanazzi, P.F., 1987. Crystal structures of lizardite-1T and lizardite-2H1 from Coli, Italy. Am Mineral 72, 943-948.

Mercier, G., Blais, J.-F., Cecchi, E., Veetil, S.P., Pasquier, L.-C., Kentish, S., 2016. Carbon dioxide chemical sequestration from industrial emissions by carbonation. Google Patents.

Moreno Correia, M.-J., 2018. Optimisation de la précipitation des carbonates de magnésium pour l'application dans un procédé de séquestration de co_2 par carbonatation minérale de la serpentine. Université du Québec, Institut national de la recherche scientifique.

Nagy, B., Faust, G.T., 1956. Serpentines: natural mixtures of chrysotile and antigorite. American Mineralogist: Journal of Earth and Planetary Materials 41, 817-838.

O'Connor, W., Dahlin, D., Rush, G., Gerdemann, S., Penner, L., Nilsen, D., 2005. Aqueous mineral carbonation. Final Report, DOE/ARC-TR-04 2.

Park, A.H.A., Fan, L.S., 2004. CO2 mineral sequestration: physically activated dissolution of serpentine and pH swing process. Chemical Engineering Science 59, 5241-5247.

Pasquier, L.C., Mercier, G., Blais, J.F., Cecchi, E., Kentish, S., 2014a. Parameters optimization for direct flue gas CO2 capture and sequestration by aqueous mineral carbonation using activated serpentinite based mining residue. Appl Geochem 50, 66-73.

Pasquier, L.C., Mercier, G., Blais, J.F., Cecchi, E., Kentish, S., 2014b. Reaction Mechanism for the Aqueous-Phase Mineral Carbonation of Heat-Activated Serpentine at Low Temperatures and Pressures in Flue Gas Conditions. Environ Sci Technol 48, 5163-5170.

Pasquier, L.C., Mercier, G., Blais, J.F., Cecchi, E., Kentish, S., 2016. Technical & economic evaluation of a mineral carbonation process using southern Quebec mining wastes for CO2 sequestration of raw flue gas with by-product recovery. Int J Greenh Gas Con 50, 147-157.

Rigopoulos, I., Delimitis, A., Ioannou, I., Efstathiou, A.M., Kyratsi, T., 2018. Effect of ball milling on the carbon sequestration efficiency of serpentinized peridotites. Miner Eng 120, 66-74.

Seifritz, W., 1990. CO2 disposal by means of silicates. Nature 345, 486.

Seipold, U., Schilling, F., 2003. Heat transport in serpentinites. Tectonophysics 370, 147-162.

Teir, S., Revitzer, H., Eloneva, S., Fogelholm, C.J., Zevenhoven, R., 2007. Dissolution of natural serpentinite in mineral and organic acids. Int J Miner Process 83, 36-46.

Turci, F., Tomatis, M., Mantegna, S., Cravotto, G., Fubini, B., 2008. A new approach to the decontamination of asbestos-polluted waters by treatment with oxalic acid under power ultrasound. Ultrason Sonochem 15, 420-427.

Turvey, C.C., Wilson, S.A., Hamilton, J.L., Southam, G., 2017. Field-based accounting of CO2 sequestration in ultramafic mine wastes using portable X-ray diffraction. Am Mineral 102, 1302-1310.

Wang, X.L., Maroto-Valer, M.M., 2011. Dissolution of serpentine using recyclable ammonium salts for CO(2) mineral carbonation. Fuel 90, 1229-1237.

Wicks, F., Whittaker, E., 1977. Serpentine textures and serpentinization. The Canadian Mineralogist 15, 459-488.

Wilson, S.A., Raudsepp, M., Dipple, G.M., 2006. Verifying and quantifying carbon fixation in minerals from serpentine-rich mine tailings using the Rietveld method with X-ray powder diffraction data. American Mineralogist 91, 1331-1341.

Yoo, K., Kim, B.-S., Kim, M.-S., Lee, J.-c., Jeong, J., 2009. Dissolution of magnesium from serpentine mineral in sulfuric acid solution. Mater Trans 50, 1225-1230.

Graphical Abstract

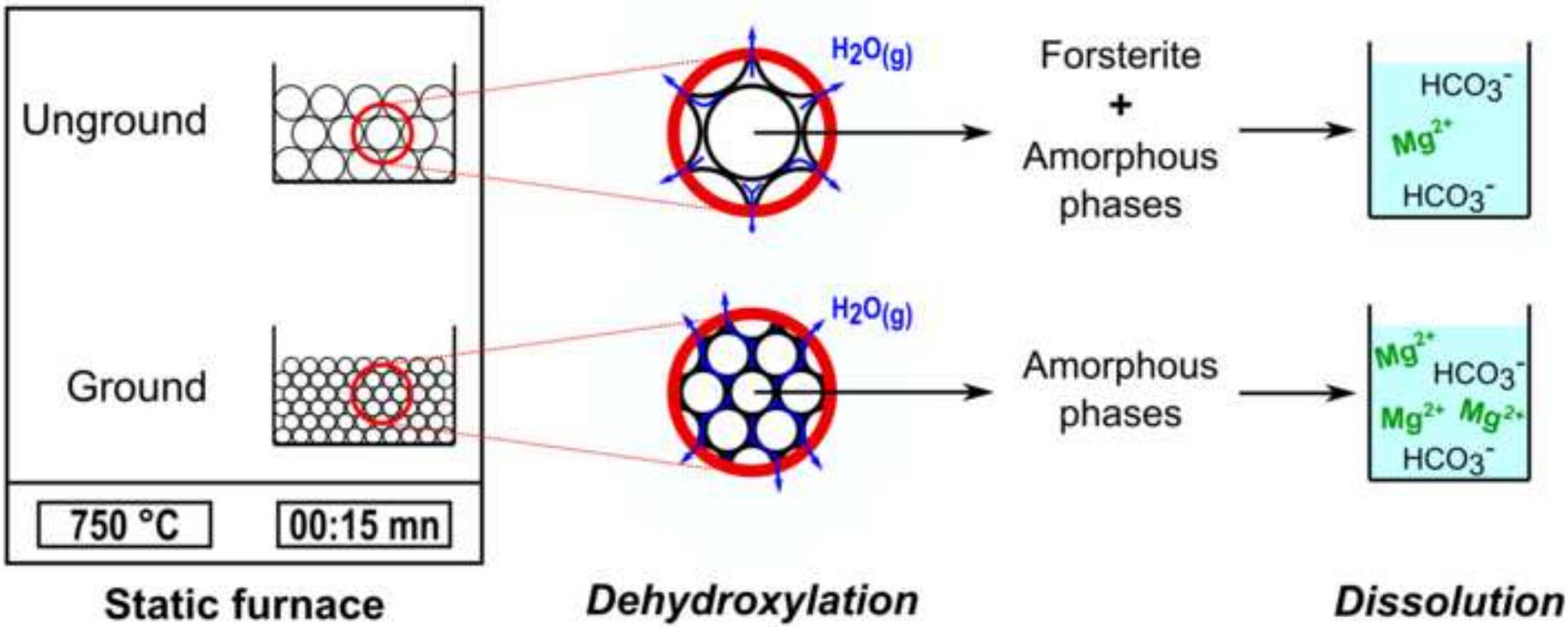

Highlights

- Thermal activation of ground and unground serpentine residues;
- Formation of amorphous phases during dehydroxylation of serpentine;
- Heating speed of ground and unground particles in serpentine residues;
- Entrapment of water vapor from removal of hydroxyl groups.

Table

Click here to download Table: Tables revised.docx

Table 1 **Chemical composition of starting material**

Elements	CaO	Cr_2O_3	Fe_2O_3	K_2O	MgO	MnO	NiO	SiO_2	LOI
wt %	0.7	0.2	6.8	0.2	41.0	0.1	0.3	39.9	13.3

Table 2 **Specific surface area of untreated samples**

Sample	Specific Surface Area ($m^2.g^{-1}$)	Standard Deviation
Untreated- Ground	19.57	0.70
Untreated- Unground	12.18	0.84

Table 3 **Mineralogical characterization of starting material: ground and unground particles**

	Ground	Unground
Measured values (Rietveld data) – wt %		
Amorphous	39.7 %	33.5 %
Serpentine	55.8 %	62.6 %
Magnetite	4.5 %	3.9 %
Calculated values– g/100g of start. mat.		
Serpentine	95.5	96.1
Magnetite	4.5	3.9

Table 4 **Mineral composition of each thermally-treated sample: ground and unground. These are expressed in grams per 100 grams of starting material**

Serp: serpentine, Inter. am: Intermediate amorphous components, Meta-serp: Meta-serpentine, Forst: Forsterite, Mag: Magnetite, Hem: Hematite, M.L.: Mass loss.

Samples	**550 °C 15 min**		**550 °C 60 min**		**650 °C 30 min**		**650 °C 60 min**		**750 °C 15 min**		**750 °C 60 min**	
Particles	G	U	G	U	G	U	G	U	G	U	G	U
Serp	53.3	74.4	53.5	62.4	21.6	25.6	4.2	22.8	0.0	5.5	0.0	0.0
Inter. Am.	36.8	14.4	37.0	19.9	60.3	38.6	70.3	34.7	49.9	42.6	34.3	43.8
Meta-serp	0.0	4.5	0.0	11.4	4.0	23.4	7.2	23.1	27.2	5.5	20.3	3.4
Forst	0.0	0.0	0.0	0.0	0.0	0.0	2.1	5.0	0.0	34.0	30.5	38.0
Mag	3.9	4.8	3.3	3.4	3.0	4.8	2.1	5.5	5.2	0.0	0.0	0.0
Hem	0.4	0.0	0.8	0.0	1.2	0.1	1.6	1.4	3.5	1.4	3.2	2.1
M.L.	5.5	2.0	5.5	3.0	9.8	7.4	12.5	7.5	14.2	10.9	11.7	12.7

Table 5 **Specific surface area ($m^2.g^{-1}$) measured on thermally-treated samples**

Samples	**Specific Surface Area ($m^2.g^{-1}$)**	**Standard Deviation**
750˚C 15 min - ground	31.04	6.72
750˚C 15 min - unground	44.94	3.45
650˚C 30 min - ground	17.15	3.11
650˚C 30 min - unground	9.48	2.83

Figure
Click here to download Figure: Figures v2 revised.docx

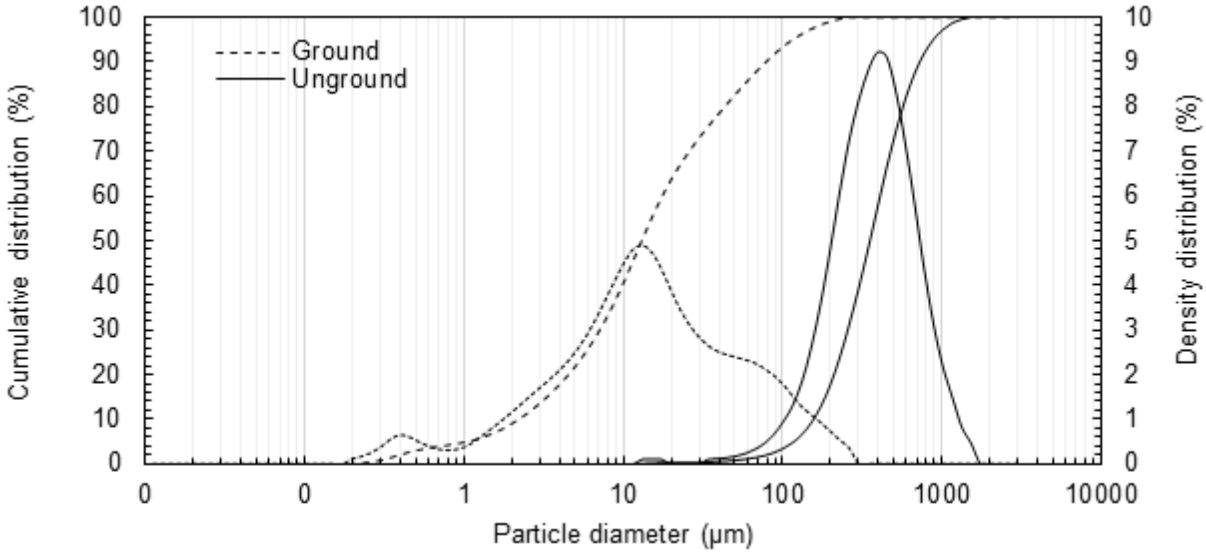

Figure 1 ***Particle size distribution of unground and ground samples***

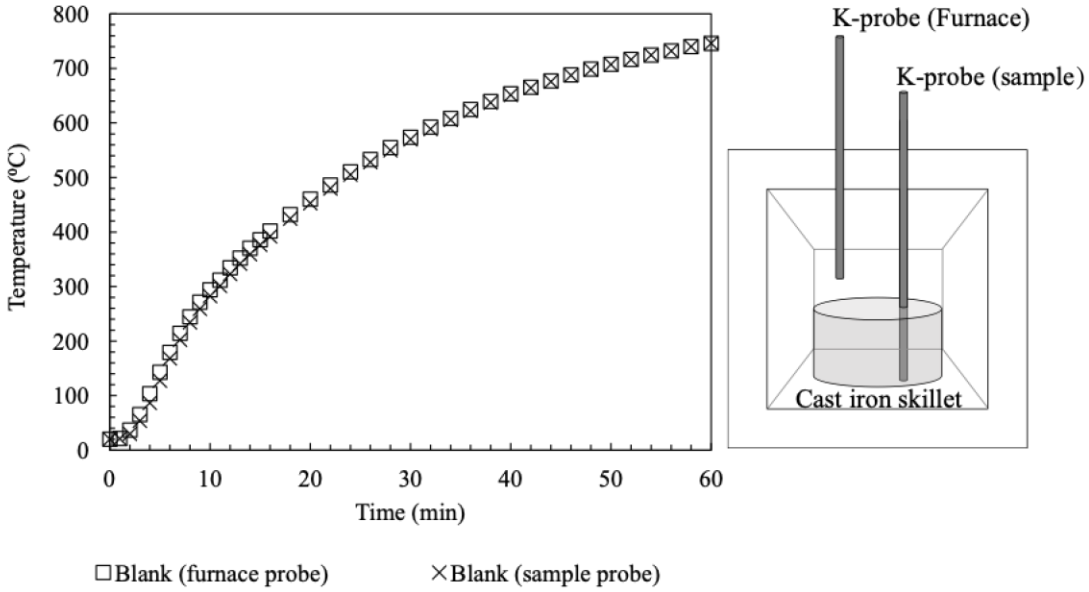

Figure 2 ***Prograde heating: calibration curve of the thermocouples***

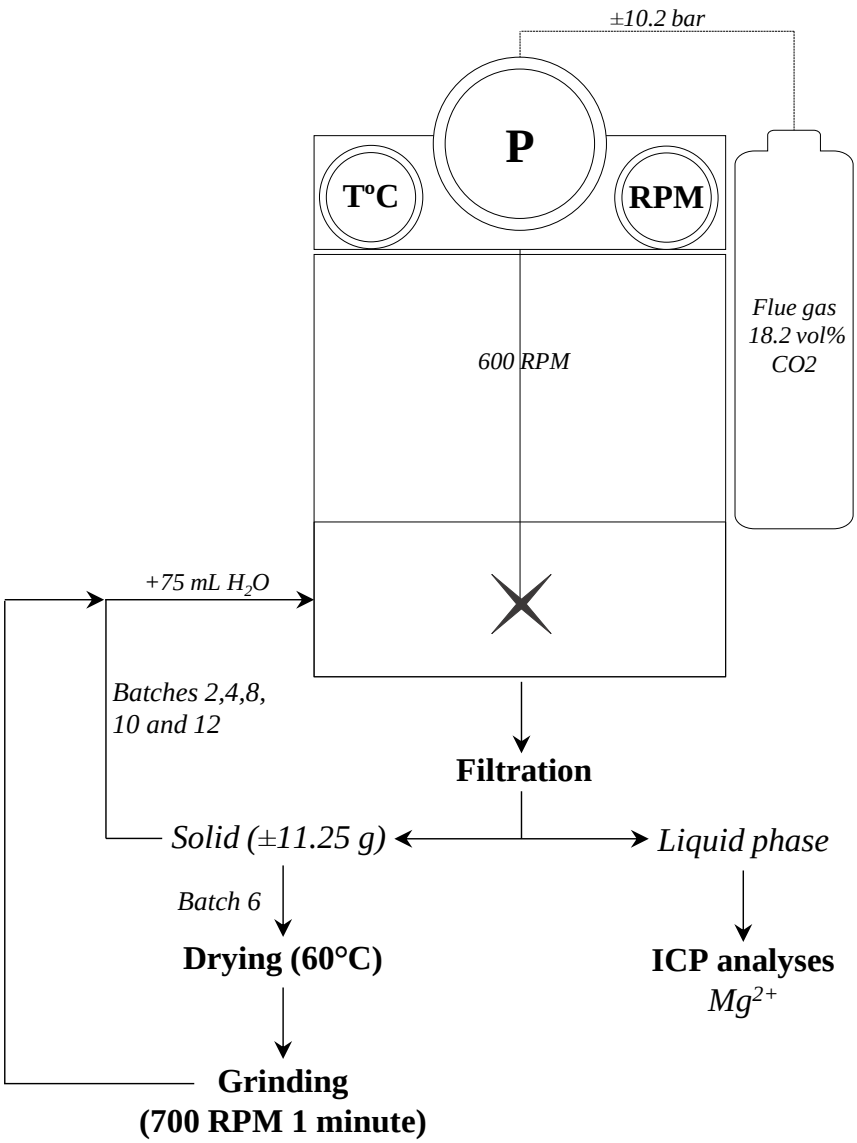

Figure 3 Dissolution experimental set-up

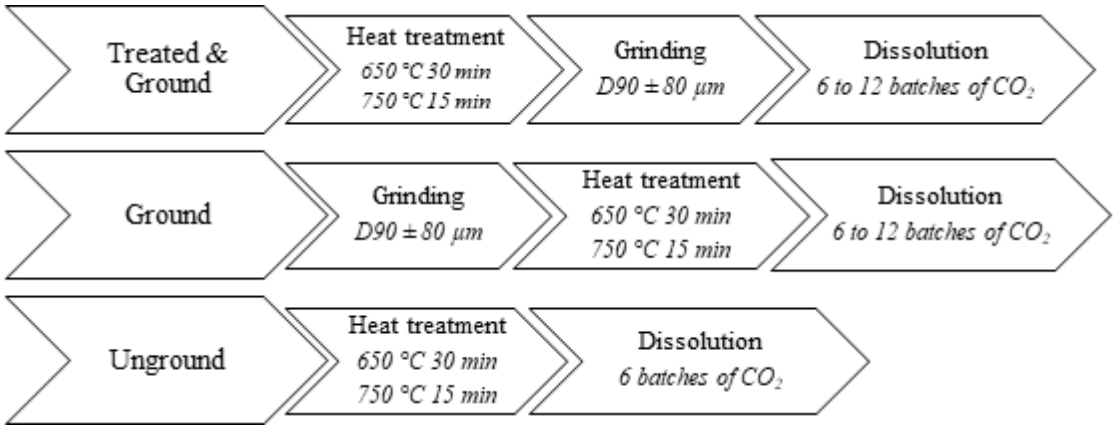

Figure 4 ***Flow sheet of experiments***

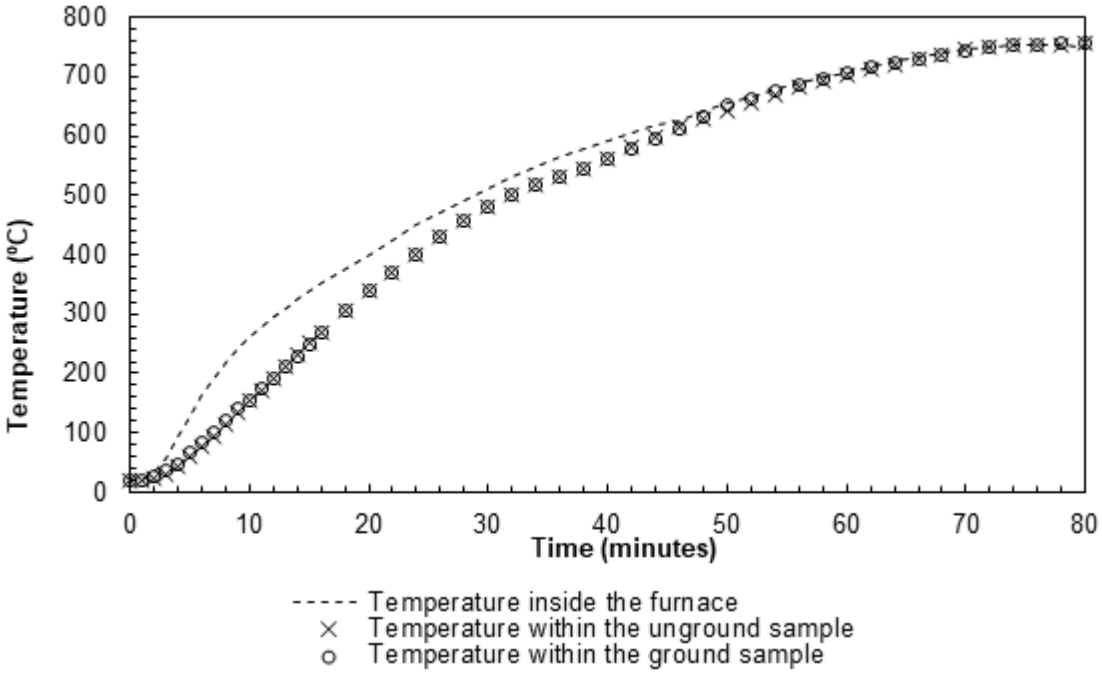

Figure 5 ***Evolution of temperatures in ground and unground samples compared to inside the furnace***

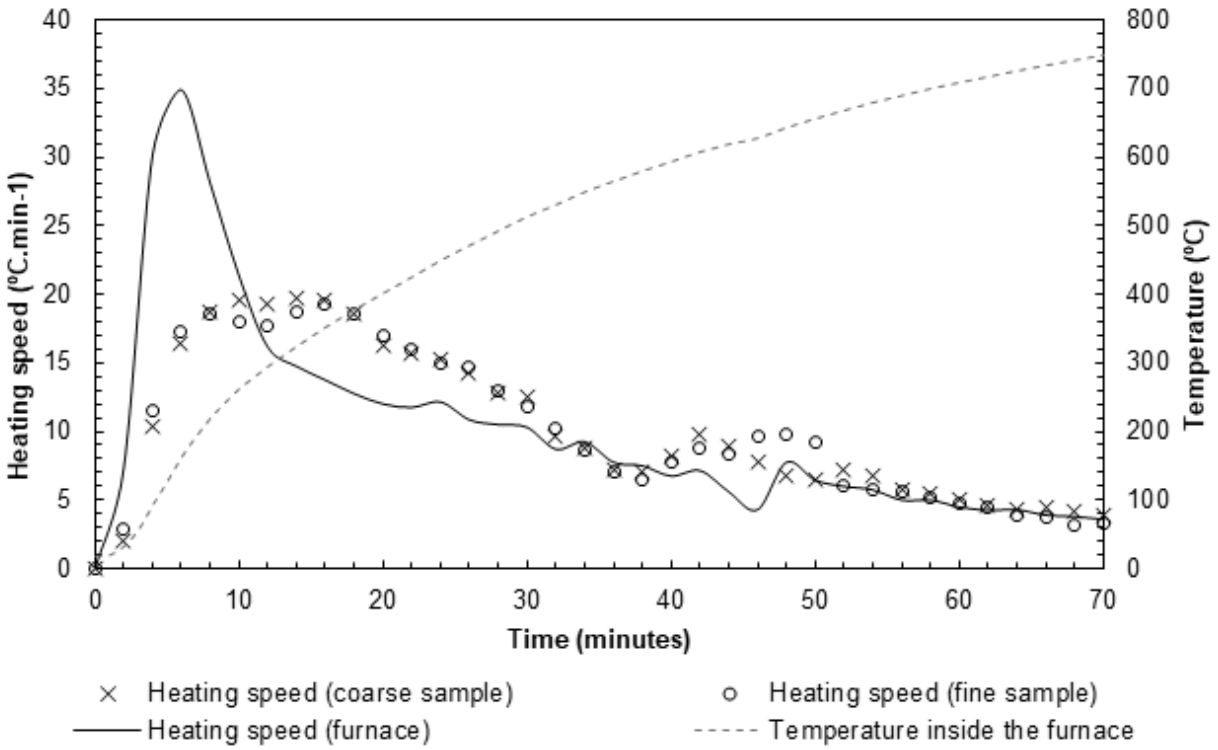

Figure 6 ***Heat diffusion expressed as heating speed between the particles in ground and unground samples***

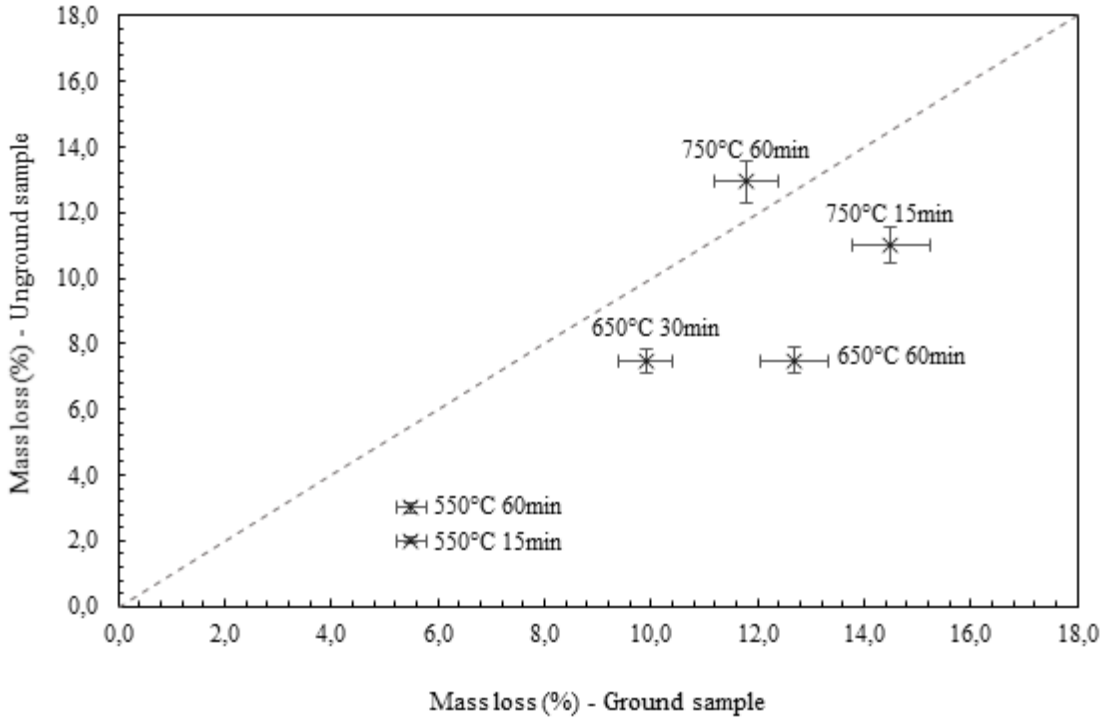

Figure 7 ***Comparison of mass lost during thermal treatment by ground and unground particles***

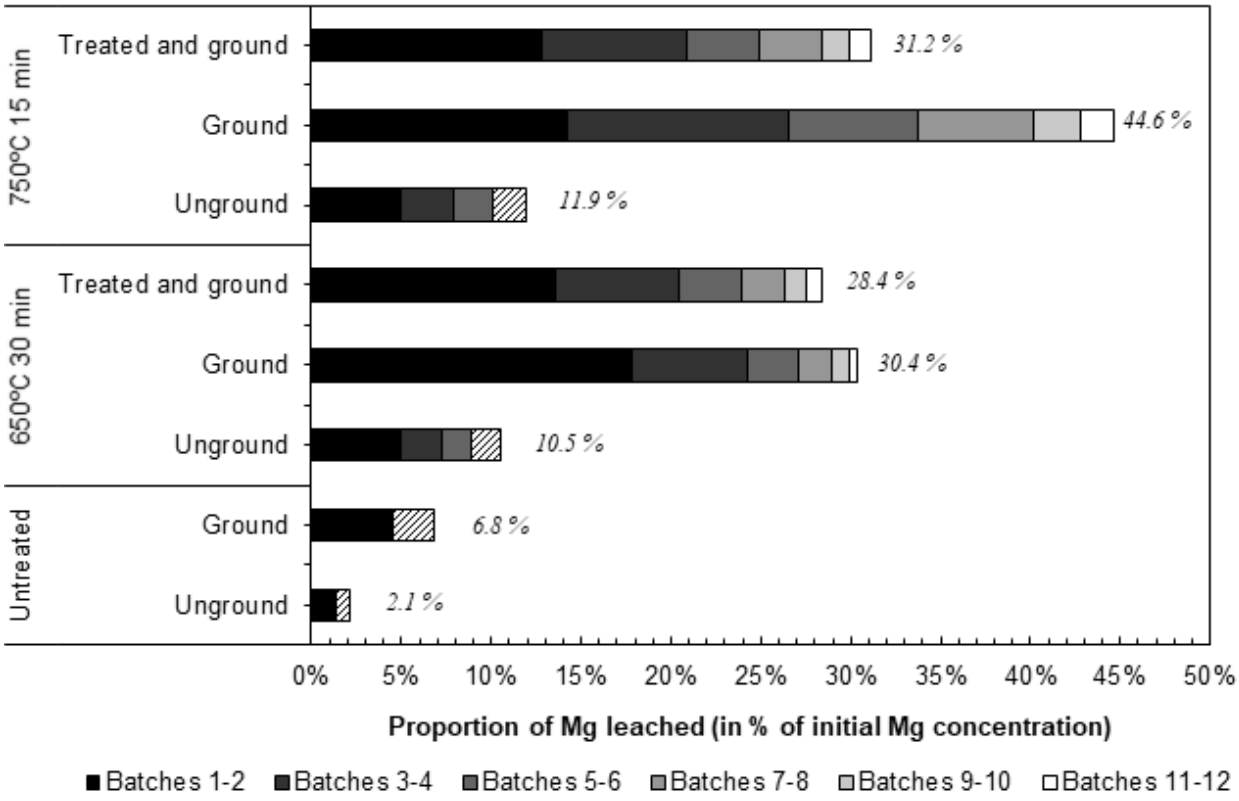

Figure 8 Proportion of Mg^{2+} extracted from 2 to 12 batches of gas carbonation

Abstract

Mineral carbonation represents a promising way of reducing the emission of anthropogenic GHG emissions, particularly in the Province of Québec where large amounts of serpentine mining residues are waiting for remediation. However, when used in reactors, serpentine minerals need to be activated to promote Mg2+ leaching. In this study, ground and unground samples have been thermally activated in a muffle furnace at different temperatures and residence times. Their mineralogical composition have been determined using XRD coupled with Rietveld refinements from which the amorphous phases have been distinguished and quantified. The objectives are to determine the influence of the particle size distribution of the samples on the dehydroxylation process and on the dissolution under aqueous mineral carbonation reaction. Results show that in a muffle furnace, unground particles tend to heat faster than ground particles. This is due to the larger spaces left between the particles, allowing a better heat diffusion through the sample. In ground particles samples, water vapor tends to be entrapped in those space, leading to the formation of a water vapor layer, slowing down the heat process. Carbonation experiments were performed on the different resulting fractions obtained. Regarding Mg dissolution efficiencies, 6 batches experiments show that Mg2+ extraction is higher when performed on sample ground prior to thermal activation. The collected information will advance the knowledge on serpentine heat activation mechanism and help to improve carbonation technologies efficiencies.

Keywords

Serpentine, Dehydroxylation, Particle Size, Heat Activation, X-Ray Diffraction, Rietveld Refinement, Magnesium Leaching, Carbonation.

Background dataset for online publication only

Click here to download Background dataset for online publication only: Supplementary Material.docx